Proceedings 2003 IEEE International Symposium on Computational Intelligence in Robotics and Automation July 16-20, 2003, Kobe, Japan

Measurement and Comparison of Human and Humanoid Walking

Satoshi Kagami[1,2], Masaaki Mochimaru[1,2], Yoshihiro Ehara[3], Natsuki Miyata[1,2], Koichi Nishiwaki[4], Takeo Kanade[1,2,5], Hirochika Inoue[4]

1 Digital Human Research Center, National Institute of Advanced Science and Technology
2 CREST Program, Japan Science and Technology Corporation(JST).
3 Teikyo University, Faculty of Medical Technology
4 The University of Tokyo, School of Information Science and Technology
5 Carnegie Mellon University, Robotics Institute

Abstract

This paper describes our research efforts aimed at understanding human being walking functions. Using motion capture system, force plates and distributed force sensors, both human being and humanoid H7 walk motion were captured. Experimental results are shown. Comparison in between human being with H7 walk in following points are discussed : 1) ZMP trajectories, 2) torso movement, 3) free leg trajectories, 4) joint angle usage, 5) joint torque usage. Furthermore, application to the humanoid robot is discussed.

1 Introduction

Recently, research on humanoid-type robots has become increasingly active, and a broad array of fundamental issues are under investigation (ex. [1,2,6,7,15]). In particular, techniques for bipedal dynamic walking, soft tactile sensors, motion planning, and 3D vision continue to progress. Humanoid robot is regarded as a general shape in human environment, its walk & balance function should be adapt to various terrain.

So far, authors have been developed biped humanoid robots and have proposed dynamically stable walking trajectory generation method based on a ZMP criteria [10, 11]. By using those system, authors have been working at low-level autonomy in humanoid autonomy by using 3D vision and motion planning [5]. However, there are many pre-defined parameters in our ZMP based walking trajectory generation, and that is a basic motivation of us to investigate human walking. Actual humanoid walking is far stable from that of human being has, therefore it can be efficient to investigate human walking.

In bio-mechatronics area, there are long history for measure and analyze human walking motion, and for example, inverted pendulum model of the walk is originaly proposed [13]. Actually motion capture system is commonly used to analyze human walking motion. There are many researches have been proposed for analyzing and comparing handicapped/aged people walking motion with normal people walking(ex. [16]).

In this paper, we use motion capture system in order to measure and investigate both our humanoid H7 and human being walking.

2 Humanoid H7

Humanoid "H7" (H:1470mm, W: 55kg) (Fig.1 left) was originally designed at JSK, University of Tokyo and it was implemented by Kawada Industries Inc. Key concept of H7 is software research platform for humanoid robot autonomy, and in order to achieve this goal, mechanical components, sensing system, and computational availability are improved [4].

2.1 A Fast ZMP Tracking Trajectory Generation Method

Since a humanoid robot has many degrees of freedom, position-based trajectory generation has been adopted mostly using a ZMP [12] constraint. Several remarkable issues have been proposed using ZMP criteria mostly applying to a walking pattern generation for a real humanoid type robot [2,3,8,14]. We proposed a fast trajectory generation method by using a relationship between robot center of gravity and ZMP.

2.2 Dynamics Model of Humanoid Type Robot

First, we introduce a model of humanoid type robot by representing motion and rotation of the center of the gravity (COG). Set z axis be the vertical axis, and x and y axis be the other component of sagittal and lateral plane respectively. Set m_i, $\boldsymbol{r}_i = (x_i, y_i, z_i)$, w_i, I_i be weight, position, angle velocity, inertia moment of $i$the link respectively. Let total mass of the robot be m_{total}, and total center of the gravity be $\boldsymbol{r}_{cog} = (r_{cog_x}, r_{cog_y}, r_{cog_z})$. Then they are represented as follows:

$$m_{total} = \sum m_i \tag{1}$$

$$r_{cog_x} = \frac{\sum m_i r_{x_i}}{m_{total}} \tag{2}$$

$$r_{cog_y} = \frac{\sum m_i r_{y_i}}{m_{total}} \tag{3}$$

$$r_{cog_z} = \frac{\sum m_i r_{z_i}}{m_{total}} \tag{4}$$

Let moment around its center of gravity be $\boldsymbol{M}_{cog}$, total force that robot obtains be $\boldsymbol{f} = (f_x, f_y, f_z)$ and total moment around a point $\boldsymbol{p} = (p_x, p_y, p_z)$ be $\boldsymbol{T}$, then dynamic equation around a point $\boldsymbol{p}$ is approximately represented as follows:

0-7803-7866-0/03/$17.00 ©2003 IEEE

$$m_{total}(\boldsymbol{r}_{cog} - \boldsymbol{p}) \times (\ddot{\boldsymbol{r}}_{cog} + \boldsymbol{g}) + \boldsymbol{M}_{cog} - \boldsymbol{T} = 0 \quad (5)$$
$$\boldsymbol{f} = m_{total}(\ddot{\boldsymbol{r}}_{cog} + \boldsymbol{g})$$

ZMP $\boldsymbol{p}_{cog} = (p_{cog_x}, p_{cog_y})$ around point $\boldsymbol{p} = (p_x, p_y, h)$ on the horizontal place $z = h$ is defined as a point where moment around point $\boldsymbol{p}$ be $\boldsymbol{T} = (0, 0, Tz)$, and it can be calculated from Equation 5.

$$p_{cog_x} = r_{cog_x} - \frac{M_{cog_y} - m_{total}(r_{cog_z} - h)(\ddot{r}_{cog_x} + g)}{m_{total}(\ddot{r}_{cog_z} + g)} \quad (6)$$
$$p_{cog_y} = r_{cog_y} - \frac{M_{cog_x} - m_{total}(r_{cog_z} - h)(\ddot{r}_{cog_y} + g)}{m_{total}(\ddot{r}_{cog_z} + g)}$$

Let $h = 0$ in Equation 6 and using Equation 5, then ZMP can be calculated as follows when desired robot motion has been achieved [9].

$$p_{cog_x} = r_{cog_x} - \frac{M_{cog_y} - m_{total} r_{cog_z}(\ddot{r}_{cog_x} + g)}{f_z} \quad (7)$$
$$p_{cog_y} = r_{cog_y} - \frac{M_{cog_x} - m_{total} r_{cog_z}(\ddot{r}_{cog_y} + g)}{f_z}$$

2.3 Stabilization by Horizontal Center of Gravity Position Modification

Let $\boldsymbol{p}^*_{cog}(t)$ be the given ideal ZMP trajectory, and $\boldsymbol{WBT}(t)$ be the whole body trajectory (ex. walking motion trajectory). When robot moves along given $\boldsymbol{WBT}(t) = \boldsymbol{r}^o(t)$, then resulting moment $\boldsymbol{M}^o$, force $\boldsymbol{f}^o$, ZMP $\boldsymbol{p}^o_{cog}$, center of gravity $\boldsymbol{r}^o_{cog}$ is calculated.

Problem statement and compensation scheme are defined as follows:

Problem Statement: For given ideal ZMP trajectory $\boldsymbol{p}^*_{cog}(t)$ and given input body trajectory $\boldsymbol{WBT}(t) = \boldsymbol{r}^o(t)$, calculate an approximate new trajectory $\boldsymbol{r}^*_{cog}(t)$ that causes a new ZMP trajectory $\boldsymbol{p}_{cog}(t)$ which is close enough to the given ideal ZMP trajectory $\boldsymbol{p}^*_{cog}(t)$.

From Equation 7, following equations is obtained for both in ideal and current $\boldsymbol{p}, \boldsymbol{r}$ respectively.

$$\begin{aligned} p_{cog_x}(t) &= r_{cog_x}(t) \\ &\quad - \frac{M^o_{cog_x}(t) - m_{total} r_{cog_z}(t)(\ddot{r}^o_{cog_x}(t) + g)}{f^o_z(t)} \quad (8) \\ p^*_{cog_x}(t) &= r^*_{cog_x}(t) \\ &\quad - \frac{M^*_{cog_x}(t) - m_{total} r^*_{cog_z}(t)(\ddot{r}^*_{cog_x}(t) + g)}{f^*_z(t)} \end{aligned}$$

Compensation Scheme: In order to simplify Equation 7, only horizontal modification of the body trajectory is considered.

Since only horizontal compensation motion of the body is considered, $r^o_{cog_z} = r^*_{cog_z}$. Then, two assumptions are introduced:

Assumption 1 We assume that effect to the force $\boldsymbol{f}(t)$ that robot obtains from its self motion is small enough. Therefore,

$$\boldsymbol{f}^o_z(t) = \boldsymbol{f}^*_z(t) \quad (9)$$

Assumption 2 We assume that effect to the torque around center of gravity that robot obtains $\boldsymbol{M}_{cog}(t)$ from its self motion is small enough. Therefore

$$\boldsymbol{M}^o(t) = \boldsymbol{M}^*(t) \quad (10)$$

With these assumptions, and let $\boldsymbol{p}^{err}_{cog}(t)$ be an error between ideal ZMP $\boldsymbol{p}^*_{cog}(t)$ and current ZMP $\boldsymbol{p}_{cog}(t)$, and $\boldsymbol{r}^{err}_{cog}(t)$ be the an error between ideal center of gravity trajectory $\boldsymbol{r}^*_{cog}(t)$ and current trajectory $\boldsymbol{r}_{cog}(t)$.

$$\begin{aligned} \boldsymbol{p}^{err}_{cog}(t) &= \boldsymbol{p}^*_{cog}(t) - \boldsymbol{p}_{cog}(t) \quad (11) \\ \boldsymbol{r}^{err}_{cog}(t) &= \boldsymbol{r}^*_{cog}(t) - \boldsymbol{r}_{cog}(t) \end{aligned}$$

Therefore following result is obtained from Equation 9 and Equation 11.

$$\boldsymbol{p}^{err}_{cog}(t) = \boldsymbol{r}^{err}_{cog}(t) - \frac{m_{total} r_{cog_z}(t) \ddot{\boldsymbol{r}}^{err}_{cog}(t)}{f^o_z(t)} \quad (12)$$

2.4 Solving Differential Equation

Equation 12 can be solved as subtract approximation. By discretizing Equation 12 with small time step Δt with iteration $i, (i = 0, 1, 2, \ldots, n-1, n)$,

$$\begin{aligned} \boldsymbol{p}^{err}_{cog}(t) &\rightarrow \boldsymbol{p}^{err}_{cog}(i) \quad (13) \\ \boldsymbol{r}^{err}_{cog}(t) &\rightarrow \boldsymbol{r}^{err}_{cog}(i) \\ \ddot{\boldsymbol{r}}^{err}_{cog}(t) &\rightarrow \frac{\boldsymbol{r}^{err}_{cog}(i+1) - 2\boldsymbol{r}^{err}_{cog}(i) + \boldsymbol{r}^{err}_{cog}(i-1)}{\Delta t^2} \end{aligned}$$

Then trinomial expression which satisfies $r^{err}_{cog}(i)$ is obtained when $1 \leq i \leq n-1$.

$$a_i \boldsymbol{r}^{err}_{cog}(i-1) + b_i \boldsymbol{r}^{err}_{cog}(i) + c_i \boldsymbol{r}^{err}_{cog}(i+1) = d_i \quad (14)$$

Here,

$$\begin{aligned} a_i &= -\frac{m_{total} r^o_{cog_z}(i)}{f^o_z(i)\Delta t^2} \quad (15) \\ b_i &= 1 + 2\frac{m_{total} r^o_{cog_z}(i)}{f^o_z(i)\Delta t^2} \\ c_i &= -\frac{m_{total} r^o_{cog_z}(i)}{f^o_z(i)\Delta t^2} \\ d_i &= p^{err}_{cog}(i) \end{aligned}$$

Then using boundary condition of trinomial expression, boundary condition $i = 0, i = n$ is calculated. In this paper, we fix terminal position. If statically stable posture is given as the terminal posture, both end of resulted trajectory will not be moving.

- Since terminal position is fixed, x_0, x_n are given.
- From position and acceleration of center of gravity relationship, number of variables is $n-1$ from $t = 1$ to $t = n - 1$.

Table 1: Comparison of Major Body Parameters

link	Human Being	Humanoid H7
Height [cm]	168.3	147.0
Weigth [kg]	61.4	53.5
Foot w[kg]	1.1	1.8
Foot l[cm]	7.3	6.0
Shank w[kg]	3.1	3.3
Shank l[cm]	39.0	30.0
Thigh w[kg]	6.6	2.9
Thigh l[cm]	35.7	30.0

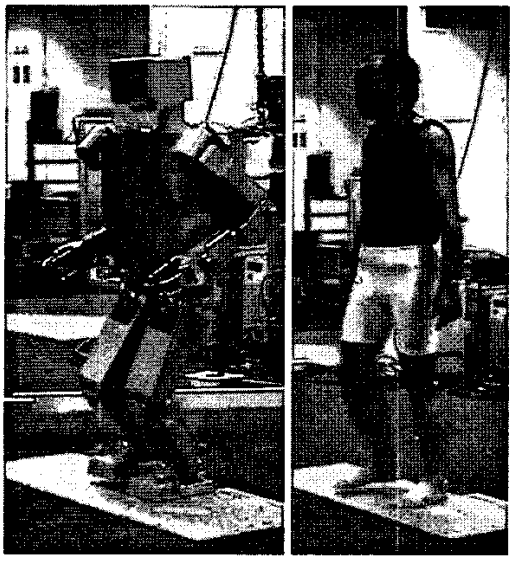

Figure 1: Motion capture scene for humanoid H7 and human being while they are walking

- From ZMP constraint, number of variables is $n+1$ from $t = 0$ to $t = n$.

As for boundary condition, terminal velocity is indefinite, we set the following boundary conditions.

$$\begin{aligned} b_0 &= b_n = 1 \\ a_0 &= a_n = 0 \\ c_0 &= c_n = 0 \end{aligned} \tag{16}$$

Given coefficient matrix, trinomial expression is solved, and discrete r_{cog}^{err} is calculated.

3 Walk Measurement and Analysis

Fig.1 shows humanoid robot H7 and human being walk in motion capture system. Table 1 shows dimensions of each subject. Motion capture system that has seven cameras is produced by Vicon, and two force plates are utilized. Analysis is done by using right side of one cycle step (from landing to end of air phase).

In order to capture human being motion, marker of the motion capture system is attached to torso, hip, knee, ankle, and foot. Hip joint is calculated 18markers. Both knee and ankle joint is assumed to be modeled by only one DOF. Those joints are parallel with each other, and it is perpendicular to the triangle of knee, ankle and foot markers. Knee joint is 2.6ankle joint is 2

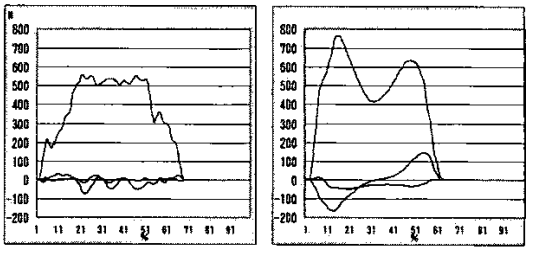

Figure 2: Three Axis Floor Reaction Force for 1 Cycle of Right Leg: H7 (left), Human (right)

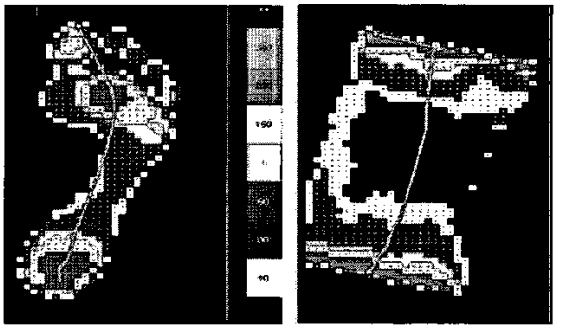

Figure 3: Distributed Floor Reaction force for 1 Cycle of Right Leg: H7 (left), Human (right)

Link weight for human being is calculated by approximating each link by cylindroid. Link weight for a robot is taken from 3D mechanical CAD data (CATIA). From floor reaction force and body parameters, inverse dynamics calculation is utilized to calculate joint moment, joint torque and joint power.

Using those link parameters and force plates, inverse dynamics calculation was applied to calculate joint torque and power.

4 Comparison

4.1 Floor Reaction Force

Three floor reaction forces are shown in Fig.2. Left side of Fig.2 shows one cycle of right leg by H7, and right side shows that of human being. F_z of H7 shows almost its weight during single support phase, and during dual leg phase F_z gradually shifts from/to the other leg. However F_z of human dual leg phase shows 20-30% heavier weight, and 20-30

As for F_x, F_y, H7 doesn't use those values because given ideal ZMP position is not moving in the foot. However human uses F_x, F_y which can be regarded that human uses frictions on the floor.

4.2 ZMP Movement

Fig.3 shows the result of foot distribution sensor and COP. According to our walking trajectory generation method mentioned in section 2., ZMP trajectory is given of the algorithm. In this paper, we gave the center point of the foot. However, human uses heel for landing and ZMP position is quickly move to the front area.

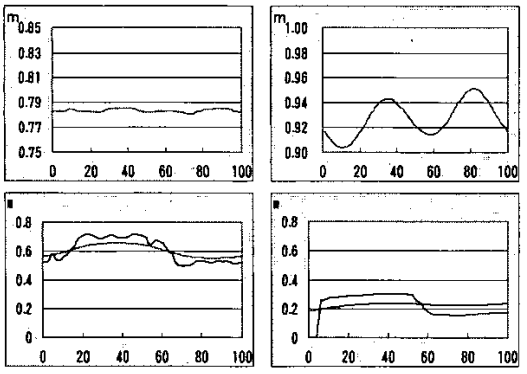

Figure 4: Sagittal Movement of Center of Gravity (upper) and Latteral Movement of CoG/CoP (lower): H7 (left), Human (right)

4.3 COG Movement

Fig.4 (upper) shows vertical movement of center of gravity (COG). H7 keeps its COG height at constant height. However, human being COG height shifts according to leg phase. The lowest height is during in dual leg phase, and the highest is during in single leg support phase.

Also, Fig.4 (lower) shows horizontal movement of COG and ZMP. H7 shifts its COG about 16cm in order to satisfy given ZMP trajectory. However, human COG movement is about 3cm, even shifting ZMP trajectory in horizontal direction.

4.4 Knee Joint Angle

Fig.5 (middle) shows knee joint angle. H7 uses knee joint for lifting up its foot at the beginning of air phase. Human bends its knee at both dual leg phase and extend at single support leg phase (double knee action). However joint angle in single support phase doesn't reach straight nor rock (hyperextension). Instead, the end of air phase, human knee joint reach about strait or rock position.

4.5 Hip Joint Moment

Fig.6 (upper) shows hip joint moment. H7 doesn't use hip joint moment since walking speed is quite small. However, human has quite remarkable two peak in both dual leg phase. Considering the other leg phase is 180[deg] different with this graph, resulted total hip joint moment will balance around yaw(Z)-axis. This symmetric usage of hip joint moment is known in biomechanical field.

5 Discussion

Since the body dynamics and actuator mechanisms of H7 and human being are not the same, qualitative analysis can be achieved. Especially energy consumption mechanisms will be quite different. There are several remarkable difference in between H7 and human walk motion.

5.1 Free Leg Trajectory

H7 lifts its free foot by using knee joint (Fig.5 middle left). Foot was kept parallel to the ground by using

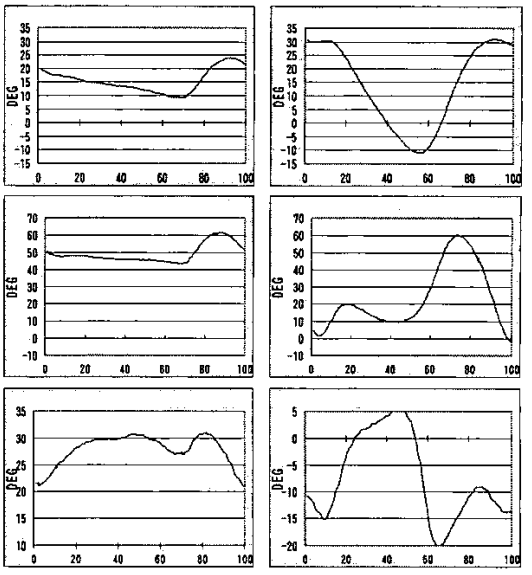

Figure 5: Hip, Knee, Ankle Pitch Joint Angle: H7 (left), Human (right)

ankle joint (Fig.5 lower left) in order to avoid collision. However, human foot angle is not always parallel to the ground. During the dual leg phase, human launch its body by using both leg (as mentioned in Section 4.5), and the accelerated body lifts the free leg. Torso roll angle was just only 2[deg] for help lifting free leg.

5.2 COG Movement

H7 doesn't move its COG in vertical direction. This is also given parameters from our walk trajectory generation method. Human COG trajectory moves in vertical direction. Vertical movement of COG doesn't have any meaning for energy consumption. However, human has small total movement of COG (around 3[cm] from the line).

Also floor reaction force F_z maximized at the dual leg phase, human can use higher friction of the ground with small disturbance around yaw-axis. Instead in single leg phase, human has equivalently small weight that causes small horizontal movement of the COG.

5.3 ZMP Trajectory Design

H7 tries to put its ZMP at center of the foot so that robot can have maximum stability for any direction. However, human being has very asymmetric ZMP trajectory for both lateral and sagittal direction.

6 Conclusion

In this paper, walking motion comparison of our humanoid robot H7 and human being is described. Since many parameters are different (including link parameters, walking speed, step length, step cycle and mechanisms), discussion about energy consumption, balance control scheme are not achieved. However, we found several interesting difference by qualitative analysis, especially 1) Free leg trajectory, 2) COG movement, and

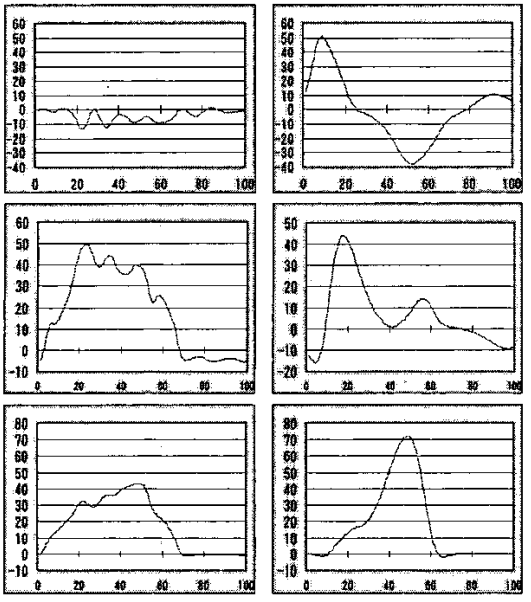

Figure 6: Hip, Knee, Ankle Pitch Joint Moment: H7 (left), Human (right)

3) ZMP trajectory design. We would like to improve humanoid walking trajectory generation method and balance compensation method by using those information.

Also those measurement system is very important for developing a humanoid walking system, since only dead-reckoning results are obtained by using onbody sensors. So we would like to use this environment for evaluate internal sensors and for develop humanoid walking function for uneven terrain.

References

[1] Rodney A. Brooks. Prospects for human level intelligence for humanoid robots. In *Proc. of the First Int. Symp. on HUmanoid RObots (HURO '96)*, pages 17–24, 1996.

[2] Kazuo HIRAI. Current and Future Perspective of Honda Humanoid Robot. In *Proc. of 1997 IEEE Intl. Conf. on Intelligent Robots and Systems (IROS'97)*, pages 500–508, 1997.

[3] S. KAGAMI, F. KANEHIRO, Y. TAMIYA, M. INABA, and H. INOUE. Autobalancer: An online dynamic balance compensation scheme for humanoid robots. In *Proc. of Fourth Intl. Workshop on Algorithmic Foundations on Robotics (WAFR'00)*, pages SA–79–SA–89, 2000.

[4] S. Kagami, K. Nishiwaki, J. J. Kuffner, Y. Kuniyoshi, M. Inaba, and H. Inoue. Design and implementation of software research platform for humanoid robotics : H7. In *Proceedings of the 2001 IEEE-RAS International Conference on Humanoid Robots*, pages 253–258, 10 2001.

[5] S. Kagami, K. Nishiwaki, J.J. Kuffner, K. Okada, M. Inaba, and H. Inoue. Low-level autonomy of remote operated humanoid robot h6 & h7. In *Preprint of 10th International Symposium of Robotics Research*, Victoria, Australia, 2001.

[6] K. Kawamura, D. M. Wiles, T. Pack, M. Bishay, and J. Barile. Humanoids: Future robots for home and factory. In *Proc. of the First Int. Symp. on HUmanoid RObots (HURO '96)*, pages 53–62, 1996.

[7] Y. Murase, K. Sakai, M. Inaba, and H. Inoue. Testbed hardware model of the hrp virtual platform. In *Proc. of '98 Annual Symposium of Robotics-Mechatronics*, pages 2P2–89–091, 1998.

[8] K. Nagasaka, M. Inaba, and H. Inoue. Walking Pattern Generation for a Humanoid Robot based on Optimal Gradient Method. In *Proc. of 1999 IEEE Int. Conf. on Systems, Man, and Cybernetics No. VI*, 1999.

[9] Ken'ichirou NAGASAKA, Masayuki INABA, and Hirochika INOUE. Research on human-based genetic motion acquisition for humanoid. In *Proc. of the 16th Annual Conf. of Robotics Society of Japan*, pages 827–828, 1998.

[10] K. Nishiwaki, S. Kagami, Y. Kuniyoshi, M. Inaba, and H. Inoue. Online Generation of Desired Walking Motion on Humanoid based on a Fast Generation Method of Motion Pattern that Follows Desired ZMP. In *19th Annual Conf. of Robotics Society of Japan (RSJ 2001)*, pages 985–986, 2001.

[11] K. NISHIWAKI, T. SUGIHARA, S. KAGAMI, M. INABA, and H. INOUE. Online Generation of Desired Walking Pattern by Dynamically Stable Mixture and Connection of Pre-designed Motions. In *18th Annual Conf. of Robotics Society of Japan (RSJ 2000)*, pages 1473–1474, 2000.

[12] Vukobratović, A.A. Frank, and D.Juričić. On the Stability of Biped Locomotion. *IEEE Trans. on Biomedical Engineering*, 17(1):25–36, 1970.

[13] W. Weber and E. Weber. *Mechanik des menschlichen*. Gehwerkzeuge, 1836.

[14] J. Yamaguchi, A. Takanishi, and I. Kato. Development of a Biped Walking Robot Compensating for Three-Axis Moment by Trunk Motion. *Journal of the Robotics Society of Japan*, 11(4):581–586, 1993.

[15] Jin'ichi Yamaguchi, Sadatoshi Inoue, Daisuke Nishino, and Atsuo Takanishi. Development of a bipedal humanoid robot having antagonistic driven joints and three dof trunk. In *Proc. of the 1998 IEEE/RSJ Int. Conf. on Intelligent Robots and Systems*, pages 96–101, 1998.

[16] N. Yamazaki. *Qualitative Evaluation of Walking Motion by using Force Plate*, pages 175–185. University of Tokyo Press, 1978.